BANCA D'ITALIA
EUROSISTEMA

Questioni di Economia e Finanza

(Occasional Papers)

Real and financial cycles: estimates using unobserved component models for the Italian economy

by Guido Bulligan, Lorenzo Burlon, Davide Delle Monache and Andrea Silvestrini

BANCA D'ITALIA
EUROSISTEMA

Questioni di Economia e Finanza

(Occasional papers)

Real and financial cycles: estimates using unobserved component models for the Italian economy

by Guido Bulligan, Lorenzo Burlon, Davide Delle Monache and Andrea Silvestrini

Number 382 – July 2017

The series Occasional Papers *presents studies and documents on issues pertaining to the institutional tasks of the Bank of Italy and the Eurosystem. The* Occasional Papers *appear alongside the* Working Papers *series which are specifically aimed at providing original contributions to economic research.*

The Occasional Papers *include studies conducted within the Bank of Italy, sometimes in cooperation with the Eurosystem or other institutions. The views expressed in the studies are those of the authors and do not involve the responsibility of the institutions to which they belong.*

The series is available online at www.bancaditalia.it .

REAL AND FINANCIAL CYCLES: ESTIMATES USING UNOBSERVED COMPONENT MODELS FOR THE ITALIAN ECONOMY

by Guido Bulligan *, Lorenzo Burlon *, Davide Delle Monache* and Andrea Silvestrini*

Abstract

In this paper we examine the empirical features of both the business and financial cycles in Italy. We employ univariate and multivariate trend-cycle decompositions based on unobserved component models. Univariate estimates highlight the different cyclical properties (persistence, duration and amplitude) of real GDP and real credit to the private sector. Multivariate estimates uncover the presence of feedback effects between the real and financial cycles. At the same time, in the most recent period (2015-2016), the multivariate approach highlights a wider output gap than that estimated by the univariate models considered in this paper.

Contents

_____

* Bank of Italy, Economic Outlook and Monetary Policy Directorate.

1 Introduction[1]

Since the global financial crisis, economic performance in the industrialised world has been generally disappointing, and the growth rate of real GDP in many developed countries has declined. This deceleration has called for potential explanations and raised questions about future prospects for global economic growth.

On the one hand, it has been argued that industrialised economies are likely to suffer from a structural surplus of saving over investment, resulting from an increasing propensity to save as well as a decreasing propensity to invest (Summers, 2014). The consequence is that excessive saving acts as a drag on demand, thus reducing economic growth and inflation. At the same time, the imbalance between saving and investment exerts a downward pressure on real interest rates. This "secular stagnation" hypothesis provides a narrative that reflects much of what has been observed in the last decades. Real interest rates are very low, demand is sluggish, and inflation is below target, just as we may expect in the presence of excess saving.

On the other hand, it has been claimed that the excessive growth in credit supply to the private sector that preceded the onset of the global financial crisis resulted in sizeable financial shocks that spilled over to the real economy. According to this interpretation, business cycle fluctuations may be largely magnified and prolonged by financial "booms and busts". This "financial cycle" hypothesis (see Borio, 2017, for a very recent summary) has inspired a lively debate on the appropriate response of monetary policy to financial imbalances: should it "lean against the financial cycle", or should it neglect it? This debate has emphasised the need to improve our understanding of financial cycles and their relationship with real cycles.

Several attempts to characterise the financial cycle may be found in the literature.

Drehmann, Borio, and Tsatsaronis (2012) have provided estimates of the US financial cycle as well as those of other selected countries, by considering credit and property prices. These authors maintain that house price and credit cycles have a longer duration than traditional business cycles. Furthermore, they observe that business cycle recessions are much deeper when they coincide with the contraction phase of the financial cycle. Borio (2012) has also studied the main characteristics of the financial cycle in advanced economies, finding that the "credit gap" – meaning the difference between the actual credit-to-GDP ratio and its long-term trend (Drehmann and Tsatsaronis, 2014) – is a useful tool for the prediction of financial crises, as well as for the evaluation of risks of systemic banking crises. A similar view is shared by Schularick and Taylor (2012), who analyse a comprehensive macro-financial historical database covering the last 150 years and conclude that financial crises should be viewed as "credit booms gone wrong" (p. 1042). Likewise, Aikman, Haldane and Nelson (2015) find that sustained growth in the credit-to-GDP ratio is strongly correlated with subsequent banking crises.

Recent studies have also explored the interactions between business and financial cycles either across countries (Claessens, Kose, and Terrones, 2012) or on a country-by-country basis (Galati et al., 2016; Rünstler and Vlekke, 2016). To our knowledge, so far only one paper has proposed a joint dating of business and credit cycles with a specific focus on Italy (Bartoletto et al., 2017), by applying a local turning-point dating algorithm to the level of real GDP and credit aggregates. An earlier work (De Bonis and Silvestrini, 2014) presented estimates of the Italian financial cycle using a dataset of historical data from 1861 to 2011. As regards output gap estimates, Zizza (2006) estimated the Italian potential output using both univariate and multivariate unobserved component models including unemployment and industrial production; Bassanetti et al. (2010) provided a comparison of univariate structural time series models, while Busetti and Caivano (2016) estimated a bivariate unobserved component model with real GDP and inflation for the

Italian economy.

Concerning the estimation approach, most studies have adopted univariate non-parametric procedures to separate the trend from its cyclical deviations, such as the turning points algorithm proposed by Bry and Boschan (1971) or the Christiano-Fitzgerald filter (Christiano and Fitzgerald, 2003). This latter belongs to the class of estimated band-pass filters, which are used to extract cycles falling within a pre-defined band of frequency: usually, 8 to 32 quarters for business cycles and 32 to 120 quarters for financial cycles. However, as stressed by Rünstler and Vlekke (2016), if the filter bands do not overlap, estimates of the two cycles are uncorrelated by construction. This is a restriction one would like to test rather than impose a priori. Alternatively, parametric trend-cycle decompositions based on unobserved component models (Harvey, 1989) have been proposed in the literature. These models decompose the observed time series into a permanent trend and other stationary components, such as a stochastic cycle and seasonal fluctuations. The cyclical dynamics are then parameterized in terms of cycle length and persistence.

In this paper, we contribute to the "financial cycle" debate by exploring the empirical features of both business and financial cycles in Italy. We use a parametric procedure based on unobserved component models, using data for Italian real GDP and real credit to the private sector covering the period from 1970:Q1 to 2016:Q3. Firstly, we apply the univariate structural time series model with stochastic cycle to both series independently, in order to identify their principal characteristics (persistence, duration, amplitude, etc.). Various sub-samples are also considered, in order to assess the stability of model parameters. We next use the multivariate structural time series model with stochastic cycle introduced by Harvey and Koopman (1997) and, more recently, adopted by both Chen et al. (2012) and Rünstler and Vlekke (2016). This allows us to model jointly real GDP and real credit dynamics and to account for interactions between the corresponding estimated cycles.

Consistently with previous studies, we find that univariate trend-cycle decompositions result in markedly different cyclical properties of real GDP and real credit in Italy. The former is characterised by relatively short cycles, while the latter follows longer cycles. Multivariate models, which deliver a joint trend-cycle decomposition for GDP and credit, unveil relevant feedback effects (measured as phase shifts) between the financial and business cycles. In particular, the joint trend-cycle decomposition suggests that the financial cycle Granger-causes the business cycle.[2] Furthermore, multivariate model estimates result in longer and wider real business cycles; this finding is consistent with the hypothesis of a financial accelerator mechanism (Bernanke, Gertler, and Gilchrist, 1996). In the most recent sample period, the multivariate model suggests that the output gap is larger than that estimated by the univariate models considered in this paper.

The rest of this paper will deal with the following issues. Section 2 illustrates the econometric framework, describing the univariate and multivariate structural time series models used in our empirical analysis. Section 3 presents trend-cycle decompositions of real GDP and credit. Section 4 concludes and suggests ideas for further research.

2 Methodology

2.1 The univariate stochastic trend plus cycle model

We consider the stochastic trend plus cycle structural time series model proposed by Harvey (1989):

$$y_t \;=\; \tau_t + \psi_t + \epsilon_t, \quad \epsilon_t \sim \mathcal{NID}(0, \sigma_\epsilon^2), \tag{1}$$

in which the univariate time series y_t ($t = 1, \ldots, n$) is thought of as being composed by a stochastic trend component τ_t, a cyclical component ψ_t and a transitory disturbance term ϵ_t normally and independently distributed, which captures the more erratic fluctuations

---

[2]Financial indicators do seem to have forecasting power for real activity, as shown in Borio and Lowe (2004), English et al. (2005), Hatzius et al. (2010), and Ng (2011).

of the data. Intervention variables, such as outliers and structural breaks, may be added to (1).

In the context of unobserved component models, trends and cycles are latent variables that have to be represented parametrically. The stochastic trend τ_t is assumed to follow a local linear trend model, such as:

$$
\begin{aligned}
\tau_{t+1} &= \tau_t + \beta_t + \xi_t, \quad \xi_t \sim \mathcal{NID}(0, \sigma_\xi^2), \\
\beta_{t+1} &= \beta_t + \zeta_t, \quad \zeta_t \sim \mathcal{NID}(0, \sigma_\zeta^2),
\end{aligned}
\tag{2}
$$

where β_t is a stochastic slope which moves up or down because of the innovation term ζ_t. The estimate of the slope represents the underlying growth rate of the trend component. The trend and the slope innovations are normally and independently distributed.

The local linear trend is a very flexible parameterization since it encompasses several alternative specifications widely employed in empirical applications. For instance, when $\sigma_\zeta^2 = 0$ and $\sigma_\xi^2 > 0$, the slope is fixed and the trend is a random walk with constant drift. In contrast, when $\sigma_\xi^2 = 0$ and $\sigma_\zeta^2 > 0$, the trend is an integrated random walk and the resulting specification is often referred to as "smooth trend" (see Harvey and Jaeger, 1993).[3]

In equation (1), we have included a stochastic cycle ψ_t, which evolves according to the following bivariate AR(1) process

$$
\begin{aligned}
\begin{bmatrix} \psi_t \\ \psi_t^* \end{bmatrix} &= \rho \begin{bmatrix} \cos\lambda & \sin\lambda \\ -\sin\lambda & \cos\lambda \end{bmatrix} \begin{bmatrix} \psi_{t-1} \\ \psi_{t-1}^* \end{bmatrix} + \begin{bmatrix} \kappa_t \\ \kappa_t^* \end{bmatrix}, \\
\begin{bmatrix} \kappa_t \\ \kappa_t^* \end{bmatrix} &\sim \mathcal{NID}\left(\begin{bmatrix} 0 \\ 0 \end{bmatrix}; \begin{bmatrix} \sigma_\kappa^2 & 0 \\ 0 & \sigma_\kappa^2 \end{bmatrix} \right),
\end{aligned}
\tag{3}
$$

where $0 < \rho < 1$ is the damping factor, $0 < \lambda < \pi$ is the frequency of the cycle (measured in radians) and ψ_t^* is an auxiliary process that only appears by construction. Being $\rho < 1$, the cycle ψ_t is stationary with $E(\psi_t) = 0$ and $\text{Var}(\psi_t) = \frac{\sigma_\kappa^2}{1-\rho^2}$, its spectral density has

---

[3]The popular Hodrick-Prescott filter is equivalent to a restricted version of the smooth trend model, in which the smoothing constant is fixed a priori in an ad-hoc way (e.g., 1600 for quarterly data).

a peak at λ, and its periodicity is $\frac{2\pi}{\lambda}$. Furthermore, it has an ARMA(2,1) reduced form representation, with roots lying in the complex plane; see Harvey (1989, p. 46).

The local linear trend model with stochastic cycle (1)-(2)-(3) has the following state space representation:

$$y_t = \begin{bmatrix} 1 & 0 & 1 & 0 \end{bmatrix} \begin{bmatrix} \tau_t \\ \beta_t \\ \psi_t \\ \psi_t^* \end{bmatrix} + \varepsilon_t, \quad \epsilon_t \sim \mathcal{NID}(0, \sigma_\epsilon^2), \tag{4}$$

$$\begin{bmatrix} \tau_{t+1} \\ \beta_{t+1} \\ \psi_{t+1} \\ \psi_{t+1}^* \end{bmatrix} = \begin{bmatrix} 1 & 1 & 0 & 0 \\ 0 & 1 & 0 & 0 \\ 0 & 0 & \rho\cos\lambda & \rho\sin\lambda \\ 0 & 0 & -\rho\sin\lambda & \rho\cos\lambda \end{bmatrix} \begin{bmatrix} \tau_t \\ \beta_t \\ \psi_t \\ \psi_t^* \end{bmatrix} + \begin{bmatrix} \xi_t \\ \zeta_t \\ \kappa_t \\ \kappa_t^* \end{bmatrix}, \quad \begin{bmatrix} \xi_t \\ \zeta_t \\ \kappa_t \\ \kappa_t^* \end{bmatrix} \sim \mathcal{NID}(\mathbf{0}, \mathbf{Q}), \tag{5}$$

where $\mathbf{Q} = diag\left(\sigma_\xi^2, \sigma_\zeta^2, \sigma_\kappa^2, \sigma_\kappa^2\right)$.

The state space representation will be used later on in Section 2.3 to carry out estimation of the unobserved components (see, e.g., Harvey, 1989; Durbin and Koopman, 2001).

2.2   The multivariate stochastic trend plus cycle model

We now present the generalization of the univariate stochastic trend plus cycle model described in Section 2.1 to the multivariate case. The multivariate stochastic cycle model has been originally proposed by Harvey and Koopman (1997) and applied, among others, by Harvey and Trimbur (2003) and Carvalho, Harvey and Trimbur (2007). It has been extended by Rünstler (2004) to account for phase shifts and more recently used by Rünstler and Vlekke (2016) for analysing the properties of business and financial cycles in the U.S. and in the five largest European economies.

We consider a $N \times 1$ vector $\boldsymbol{y}_t$, observed over the period $t = 1, \ldots, n$, which can be decomposed as:

$$\boldsymbol{y}_t = \boldsymbol{\tau}_t + \boldsymbol{\psi}_t + \boldsymbol{\epsilon}_t, \quad \boldsymbol{\epsilon}_t \sim \mathcal{NID}(\mathbf{0}, \boldsymbol{\Sigma}_\epsilon), \tag{6}$$

in which $\boldsymbol{\tau}_t$ is a $N \times 1$ vector of stochastic trend components while $\boldsymbol{\psi}_t$ is a $N \times 1$ vector of a cyclical components. The $N \times 1$ vector $\boldsymbol{\epsilon}_t$ contains the irregular components. It is normally and independently distributed with mean-zero vector and $N \times N$ non-negative definite covariance matrix $\boldsymbol{\Sigma}_\epsilon$.

The stochastic component $\boldsymbol{\tau}_t$ is modelled as a multivariate local linear trend model:

$$
\begin{aligned}
\boldsymbol{\tau}_{t+1} &= \boldsymbol{\tau_t} + \boldsymbol{\beta}_t + \boldsymbol{\xi}_t, \quad \boldsymbol{\xi}_t \sim \mathcal{NID}(\mathbf{0}, \boldsymbol{\Sigma}_\xi), \\
\boldsymbol{\beta}_{t+1} &= \boldsymbol{\beta}_t + \boldsymbol{\zeta}_t, \quad \boldsymbol{\zeta}_t \sim \mathcal{NID}(\mathbf{0}, \boldsymbol{\Sigma}_\zeta),
\end{aligned}
\tag{7}
$$

where $\boldsymbol{\Sigma}_\xi$ and $\boldsymbol{\Sigma}_\zeta$ are $N \times N$ non-negative definite covariance matrices and $E(\boldsymbol{\xi}_t \boldsymbol{\zeta}'_{t-s}) = \mathbf{0}$ $\forall s$. When $\boldsymbol{\Sigma}_\zeta = \mathbf{0}$ and $\boldsymbol{\Sigma}_\xi$ is positive definite, each trend is a random walk with drift. When $\boldsymbol{\Sigma}_\zeta$ is positive definite and $\boldsymbol{\Sigma}_\xi = \mathbf{0}$, we have a $N \times 1$ vector of integrated random walks. The innovations may be correlated across the N units and accordingly the $\boldsymbol{\Sigma}_\xi$ and $\boldsymbol{\Sigma}_\zeta$ matrices contain the contemporaneous covariance structure of the different levels and slopes, respectively.[4]

The elements of the vector $\boldsymbol{\psi}_t = [\psi_{1,t}, \ldots, \psi_{N,t}]'$ are modelled as stochastic cycles, with $i = 1, \ldots, N$:

$$
\begin{aligned}
\begin{bmatrix} \psi_{i,t} \\ \psi^*_{i,t} \end{bmatrix} &= \rho_i \begin{bmatrix} \cos \lambda_i & \sin \lambda_i \\ -\sin \lambda_i & \cos \lambda_i \end{bmatrix} \begin{bmatrix} \psi_{i,t-1} \\ \psi^*_{i,t-1} \end{bmatrix} + \begin{bmatrix} \kappa_{i,t} \\ \kappa^*_{i,t} \end{bmatrix}, \\
\begin{bmatrix} \kappa_{i,t} \\ \kappa^*_{i,t} \end{bmatrix} &\sim \mathcal{NID} \left(\begin{bmatrix} 0 \\ 0 \end{bmatrix}; \begin{bmatrix} \sigma^2_{i,\kappa} & 0 \\ 0 & \sigma^2_{i,\kappa} \end{bmatrix} \right),
\end{aligned}
\tag{8}
$$

where $\boldsymbol{\psi}^*_t = \left[\psi^*_{1,t}, \ldots, \psi^*_{N,t} \right]'$, $0 < \rho_i < 1$ are the damping factors and $0 < \lambda_i < \pi$ are the cycle frequencies, measured in radians.[5] Correlations across innovations driving the individual cycles are allowed via the N-dimensional covariance matrix $\boldsymbol{\Sigma}_\kappa$. Specifically, the vector of innovations $\tilde{\boldsymbol{\kappa}}_t = (\boldsymbol{\kappa}'_t, \boldsymbol{\kappa}^{*'}_t)' \sim \mathcal{NID}(\mathbf{0}, \boldsymbol{I}_2 \otimes \boldsymbol{\Sigma}_\kappa)$.

---

[4]This specification is commonly referred to as "Seemingly Unrelated Time Series Equations" (SUTSE); see Harvey (1989, Chapter 8).

[5]Under the restriction $\rho_i = \rho$ and $\lambda_i = \lambda \,\forall i$, the model features "similar cycles" (Harvey and Koopman, 1997).

Rünstler (2004) proposes to model the multivariate cycle as

$$\tilde{\boldsymbol{\psi}}_t = [\boldsymbol{A}, \boldsymbol{A}^*] \begin{bmatrix} \boldsymbol{\psi}_t \\ \boldsymbol{\psi}_t^* \end{bmatrix}, \tag{9}$$

where $\boldsymbol{A}$ and $\boldsymbol{A}^*$ are arbitrary $N \times N$ matrices such that the cyclical components are expressed as linear combinations of N independent stochastic cycles. Indeed, $\tilde{\boldsymbol{\psi}}_t$ loads on N distinct independent stochastic cycles with potentially different dynamics. At the same time, this specification allows to introduce phase shifts among cyclical components and therefore cross covariances among cycles which are shifted in time with respect to one another.

We now turn to the state space representation, which will be used in Section 2.3 for parameter estimation. For the sake of simplicity, we consider the bivariate case with $N = 2$. Then, the multivariate stochastic cycle model in (6)-(7)-(8)-(9) can be represented as:

$$\begin{bmatrix} y_{1,t} \\ y_{2,t} \end{bmatrix} = \begin{bmatrix} 1 & 0 & 0 & 0 & a_{11} & a_{12} & a_{11}^* & a_{12}^* \\ 0 & 1 & 0 & 0 & a_{21} & a_{22} & a_{21}^* & a_{22}^* \end{bmatrix} \begin{bmatrix} \tau_{1,t} \\ \tau_{2,t} \\ \beta_{1,t} \\ \beta_{2,t} \\ \hline \psi_{1,t} \\ \psi_{2,t} \\ \psi_{1,t}^* \\ \psi_{2,t}^* \end{bmatrix} + \begin{bmatrix} \varepsilon_{1,t} \\ \varepsilon_{2,t} \end{bmatrix}, \tag{10}$$

$$\begin{bmatrix} \tau_{1,t+1} \\ \tau_{2,t+1} \\ \beta_{1,t+1} \\ \beta_{2,t+1} \\ \hline \psi_{1,t+1} \\ \psi_{2,t+1} \\ \psi_{1,t+1}^* \\ \psi_{2,t+1}^* \end{bmatrix} = \begin{bmatrix} \begin{array}{cccc} 1 & 0 & 1 & 0 \\ 0 & 1 & 0 & 1 \\ 0 & 0 & 1 & 0 \\ 0 & 0 & 0 & 1 \end{array} & \boldsymbol{0}_{4,4} \\ \hline \boldsymbol{0}_{4,4} & \boldsymbol{C} \end{bmatrix} \begin{bmatrix} \tau_{1,t} \\ \tau_{2,t} \\ \beta_{1,t} \\ \beta_{2,t} \\ \hline \psi_{1,t} \\ \psi_{2,t} \\ \psi_{1,t}^* \\ \psi_{2,t}^* \end{bmatrix} + \begin{bmatrix} \xi_{1,t} \\ \xi_{2,t} \\ \zeta_{1,t} \\ \zeta_{2,t} \\ \hline \kappa_{1,t} \\ \kappa_{2,t} \\ \kappa_{1,t}^* \\ \kappa_{2,t}^* \end{bmatrix}, \tag{11}$$

with

$$\boldsymbol{C} := \begin{bmatrix} \rho_1 \cos \lambda_1 & 0 & \rho_1 \sin \lambda_1 & 0 \\ 0 & \rho_2 \cos \lambda_2 & 0 & \rho_2 \sin \lambda_2 \\ -\rho_1 \sin \lambda_1 & 0 & \rho_1 \cos \lambda_1 & 0 \\ 0 & -\rho_2 \sin \lambda_2 & 0 & \rho_2 \cos \lambda_2 \end{bmatrix}. \tag{12}$$

where $E(\boldsymbol{\epsilon}_t \boldsymbol{\epsilon}_t') = \boldsymbol{\Sigma}_\epsilon$, $E(\boldsymbol{\xi}_t \boldsymbol{\xi}_t') = \boldsymbol{\Sigma}_\xi$, $E(\boldsymbol{\zeta}_t \boldsymbol{\zeta}_t') = \boldsymbol{\Sigma}_\zeta$, $E(\boldsymbol{\kappa}_t \boldsymbol{\kappa}_t') = E(\boldsymbol{\kappa}_t^* \boldsymbol{\kappa}_t^{*\prime}) = \boldsymbol{\Sigma}_\kappa$, $E(\boldsymbol{\kappa}_t \boldsymbol{\kappa}_t^{*\prime}) = \boldsymbol{0}$.

For estimation purposes, identifying restrictions on the elements of $\boldsymbol{A}$ and $\boldsymbol{A}^*$ matrices have to be imposed. Specifically, when considering similar cycles ($\rho_i = \rho$ and $\lambda_i = \lambda \; \forall i$), we require $a_{ij} = 0$ for $i < j$ and $a_{ij}^* = 0$ for $i \leq j$ (Rünstler, 2004). With non-similar cycles, it is sufficient to impose a normalization of phase shifts, which can be achieved setting $a_{ii}^* = 0$ ($i = 1, 2, \ldots, N$) (Rünstler and Vlekke, 2016).

This delivers the following vector of cyclical components:

$$\begin{bmatrix} \tilde{\psi}_{1,t} \\ \tilde{\psi}_{2,t} \end{bmatrix} = \begin{bmatrix} a_{11}\psi_{1t} + a_{12}\psi_{2t} + a_{12}^*\psi_{2t}^* \\ a_{21}\psi_{1t} + a_{22}\psi_{2t} + a_{21}^*\psi_{1t}^* \end{bmatrix}. \tag{13}$$

It is straightforward to see that both cycles are a linear combination of three stochastic components. Specifically, the coefficients a_{ij} load the contemporaneous relationships, while the coefficients a_{ij}^* load the phase shifts. Those coefficients allow the interaction (contemporaneous and lagged) among stochastic cycles with potentially different features.

2.3 Estimation, filtering and smoothing

Consider the following linear Gaussian state space model:

$$\begin{aligned} \boldsymbol{y}_t &= \boldsymbol{Z}\boldsymbol{\alpha}_t + \boldsymbol{\varepsilon}_t, & \boldsymbol{\varepsilon}_t &\sim \mathcal{N}(\boldsymbol{0}, \boldsymbol{H}), \\ \boldsymbol{\alpha}_{t+1} &= \boldsymbol{T}\boldsymbol{\alpha}_t + \boldsymbol{\eta}_t, & \boldsymbol{\eta}_t &\sim \mathcal{N}(\boldsymbol{0}, \boldsymbol{Q}), \quad t = 1, \ldots, n, \end{aligned} \tag{14}$$

where $\boldsymbol{y}_t$ is the $N \times 1$ vector of observed variables, $\boldsymbol{\varepsilon_t}$ is the $N \times 1$ vector of measurement errors, $\boldsymbol{\alpha}_t$ is the $m \times 1$ vector of state variables and $\boldsymbol{\eta}_t$ is the corresponding $m \times 1$ vector of innovations. The two innovation vectors are assumed to be Gaussian distributed and uncorrelated for all time periods, that is, $E(\boldsymbol{\varepsilon}_t \boldsymbol{\eta}_s') = \boldsymbol{0} \; \forall t, s$.[6] The initial value of the state vector is also assumed to be Gaussian $\alpha_1 \sim \mathcal{N}(\boldsymbol{a}_1, \boldsymbol{P}_1)$ and uncorrelated $\forall t$ with $\boldsymbol{\varepsilon}$ and $\boldsymbol{\eta}$.

---

[6]This assumption can be relaxed at the cost of a slight complication in some of the filtering formulae.

Conditional on the information set $\boldsymbol{Y}_{t-1} = \{\boldsymbol{y}_{t-1}, ..., \boldsymbol{y}_1\}$ and on the vector of parameters $\boldsymbol{\theta}$, the observations and the state vector are Gaussian, i.e., $\boldsymbol{y}_t|(\boldsymbol{Y}_{t-1}; \boldsymbol{\theta}) \sim \mathcal{N}(\boldsymbol{Z}\boldsymbol{a}_t, \boldsymbol{F}_t)$ and $\boldsymbol{\alpha}_t|(\boldsymbol{Y}_{t-1}; \boldsymbol{\theta}) \sim \mathcal{N}(\boldsymbol{a}_t, \boldsymbol{P}_t)$. It follows that the log-likelihood function at time t is:

$$\ell_t = \log p(\boldsymbol{y}_t|(\boldsymbol{Y}_{t-1}, \boldsymbol{\theta})) \propto -\frac{1}{2}\left(\log|\boldsymbol{F}_t| + \boldsymbol{v}_t'\boldsymbol{F}_t^{-1}\boldsymbol{v}_t\right). \tag{15}$$

The prediction error $\boldsymbol{v}_t$, its covariance matrix $\boldsymbol{F}_t$, the state vector conditional mean $\boldsymbol{a}_t$, and its mean square error (MSE) matrix $\boldsymbol{P}_t$ are estimated optimally[7] by means of the Kalman Filter:

$$\begin{array}{ll}
\boldsymbol{v}_t = \boldsymbol{y}_t - \boldsymbol{Z}\boldsymbol{a}_t, & \boldsymbol{a}_{t+1} = \boldsymbol{T}\boldsymbol{a}_t + \boldsymbol{K}_t\boldsymbol{v}_t, \\
\boldsymbol{F}_t = \boldsymbol{Z}\boldsymbol{P}_t\boldsymbol{Z}' + \boldsymbol{H}, & \boldsymbol{P}_{t+1} = \boldsymbol{T}\boldsymbol{P}_t\boldsymbol{L}_t' + \boldsymbol{Q}, \\
\boldsymbol{K}_t = \boldsymbol{T}\boldsymbol{P}_t\boldsymbol{Z}'\boldsymbol{F}_t^{-1}, & \boldsymbol{a}_{t|t} = \boldsymbol{a}_t + \boldsymbol{P}_t\boldsymbol{Z}'\boldsymbol{F}_t^{-1}\boldsymbol{v}_t \\
\boldsymbol{L}_t = \boldsymbol{T} - \boldsymbol{K}_t\boldsymbol{Z}, & \boldsymbol{P}_{t|t} = \boldsymbol{P}_t - \boldsymbol{P}_t\boldsymbol{Z}'\boldsymbol{F}_t^{-1}\boldsymbol{Z}\boldsymbol{P}_t, \quad t = 1, \ldots, n,
\end{array} \tag{16}$$

with initial values $\boldsymbol{a}_1$ and $\boldsymbol{P}_1$.[8] Once the vector of parameters $\boldsymbol{\theta}$ is estimated by Maximum Likelihood (ML) using the prediction error decomposition of the likelihood provided by the Kalman Filter, the unobserved components can be extracted from the observations using the *predictive* filter and the associated *smoother*.

The vector $\boldsymbol{a}_t = E(\boldsymbol{\alpha}_t|(\boldsymbol{Y}_{t-1}, \boldsymbol{\theta}))$ is the so-called *predictive* filter and $\boldsymbol{P}_t = E[(\boldsymbol{a}_t - \boldsymbol{\alpha}_t)(\boldsymbol{a}_t - \boldsymbol{\alpha}_t)']$ is the associated MSE, while the *real-time* filter is $\boldsymbol{a}_{t|t} = E(\boldsymbol{\alpha}_t|(\boldsymbol{Y}_t, \boldsymbol{\theta}))$ and its MSE is $\boldsymbol{P}_{t|t} = E[(\boldsymbol{a}_{t|t} - \boldsymbol{\alpha}_t)(\boldsymbol{a}_{t|t} - \boldsymbol{\alpha}_t)']$. It is worth stressing that in this linear model the MSEs are independent from the observations, thus they are also the unconditional covariance matrices associated with the conditional mean estimators; see Harvey (1989, sec. 3.2.3).

The *smoother* algorithm allows us to estimate the state vector given all the available information, namely $\boldsymbol{a}_{t|n} = E(\boldsymbol{\alpha}_t|(\boldsymbol{Y}_n, \boldsymbol{\theta}))$ and the associated MSE $\boldsymbol{P}_{t|n} = E[(\boldsymbol{a}_{t|n} - \boldsymbol{\alpha}_t)(\boldsymbol{a}_{t|n} - \boldsymbol{\alpha}_t)']$. It is a backward recursion:

$$\begin{array}{ll}
\boldsymbol{r}_{t-1} = \boldsymbol{Z}'\boldsymbol{F}_t^{-1}\boldsymbol{v}_t + \boldsymbol{L}_t'\boldsymbol{r}_t, & \boldsymbol{N}_{t-1} = \boldsymbol{Z}'\boldsymbol{F}_t^{-1}\boldsymbol{Z} + \boldsymbol{L}_t'\boldsymbol{N}_t\boldsymbol{L}_t, \\
\boldsymbol{a}_{t|n} = \boldsymbol{a}_t + \boldsymbol{P}_t\boldsymbol{r}_{t-1}, & \boldsymbol{P}_{t|n} = \boldsymbol{P}_t - \boldsymbol{P}_t\boldsymbol{N}_{t-1}\boldsymbol{P}_t, \quad t = n, \ldots, 1.
\end{array} \tag{17}$$

with initial values $\boldsymbol{r}_n = \boldsymbol{0}$ and $\boldsymbol{N}_n = \boldsymbol{0}$.

---

[7]Producing the minimum mean squared linear estimator (MMSLE) of the state vector.

[8]See the original papers by Kalman (1960) and Kalman and Bucy (1961).

3 Empirical results

In this section we present the main characteristics of real and financial cycles in Italy. In Sections 3.1 and 3.2 we will focus on univariate trend-cycle decompositions. The analysis is preliminary to the multivariate one, as it highlights peculiarities and commonalities between real and financial cycles, based on visual inspection of the estimated cyclical components. This information is exploited in setting up and estimating the bivariate model in Section 3.3.

3.1 Univariate trend-cycle decompositions for GDP

We fit the univariate local linear trend model plus stochastic cycle in equations (1)-(2)-(3) to real GDP for Italy. In particular, we use the integrated random walk specification ($\sigma_\xi^2 = 0$ and $\sigma_\zeta^2 > 0$), which delivers a smooth trend function. The sample period is 1970:Q1-2016:Q3 and estimation is conducted via the method of Maximum Likelihood.

Figure 1 reports the smoothed estimates resulting from maximization of the likelihood, with their approximate 95% confidence intervals. The estimated cyclical component is characterised by 11 full cycles from peak to peak. While the main peaks and troughs align well with the official dating produced by ISCO-ISAE-ISTAT, the resulting cyclical component is also characterised by several additional cycles: in particular, one complete cycle (from peak to peak) in the late Eighties, one in the late Nineties, and the cyclical peak soon after 2010. However, the recovery recorded in 2010 was too feeble and short-lived to qualify as a cyclical peak, also in light of the depth of the previous recession. More technically, we find that the estimated value of λ is consistent with a cycle length of 14 quarters – in line with findings reported in Zizza (2006) – and the amplitude of the resulting cycles is always comprised between +2 and -2 percent, with the exception of the early 1970s and the 2009–2012 cycles.

Figure 1: Real GDP: Smoothed estimates of trend, slope and cycle
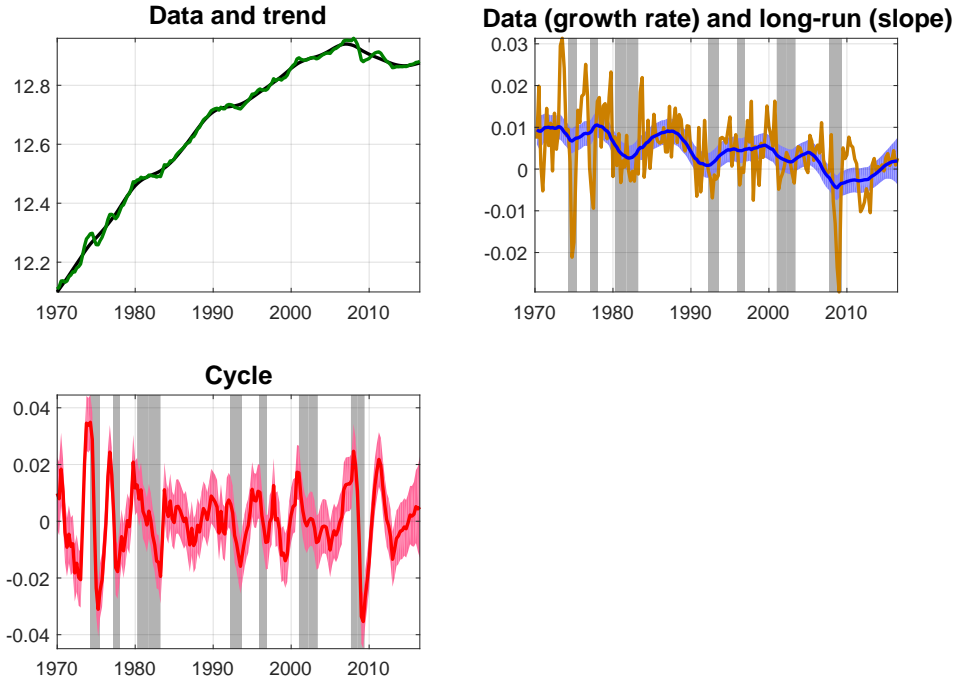
Data and trend

Data (growth rate) and long-run (slope)

Cycle

The estimated model is the integrated random walk trend plus stochastic cycle in equations (1)-(2)-(3). The sample period is 1970:Q1-2016:Q3. The variance of the irregular component is estimated to be zero, thus we impose $\sigma_\epsilon^2 = 0$. The first graph on the top left displays the data (in levels) and the estimated trend. The first graph on the top right shows the data in first differences (quarterly growth rate) and the estimated slope with 95% confidence intervals. The bottom panel displays the estimated cycle with 95% confidence intervals. Recessions are highlighted by grey shaded areas.

Overall, the estimation of the univariate model leads to short cyclical fluctuations with little or no difference in amplitude across cycles. This last feature can be better appreciated turning our attention to the resulting trend (slope) component of GDP in Figure 1, which can be economically interpreted as the long-run potential growth of the economy. The latter shows a significant degree of volatility, which is reflected in periods of increasing and decreasing potential growth. On the one hand, the pro-cyclicality of the estimated trend component explains why the cycle amplitude does not vary significantly

16

over time. On the other hand, it suggests the presence of some residual cyclicality in the trend component, perhaps due to a longer cycle uncorrelated with the one uncovered so far.

The resulting decomposition obtained at the likelihood's global maximum resembles what could be obtained using the Hodrick-Prescott filter. This result confirms Zizza's (2006) findings and Busetti and Caivano's (2016) earlier analysis, with the caveat that the global maximum we find seems to coincide with their local maximum. In order to investigate whether our results are driven by the choice of the initial conditions and by the presence of multiple local maxima, we perform a recursive estimation of model parameters (ρ, λ, σ_ζ^2, and σ_κ^2) based on expanding-window (partial samples of increasing size). The expanding-window estimation starts in 2000:Q1. The size of the first window is therefore 121 quarterly observations, i.e., approximately 30 years of data, while the final window coincides with the full sample period, 1970:Q1-2016:Q3. Starting from two different initial values of λ ($2\pi/20$ and $2\pi/40$), Figure 2 shows that the ML estimation procedure selects the same optimal parameters throughout the sample period (i.e., the blue and orange line overlap). Also the evolution over time of parameter estimates shows only limited upward movements from 2009-2010 onwards. The likelihood function is well shaped throughout the sample and does not point to the presence of multiple local maxima nor to significant time variation.[9]

---

[9]We also performed a rolling window exercise whereby at each iteration a new data point is added and the oldest data point discarded so as to maintain the length of the estimation window fixed. While this set-up tends to magnify time variation, we reached very similar conclusions to those reported in the main text. The only exception are the estimates based on sample windows including the period between the early 80's and 2008 when the likelihood function shows two maxima, one local at $\lambda = 0.48$ (period ≈ 13 quarters) and one global at $\lambda = 0.15$ (period ≈ 40 quarters), confirming Busetti and Caivano's findings.

Figure 2: Real GDP: Parameter instability analysis based on an expanding estimation window
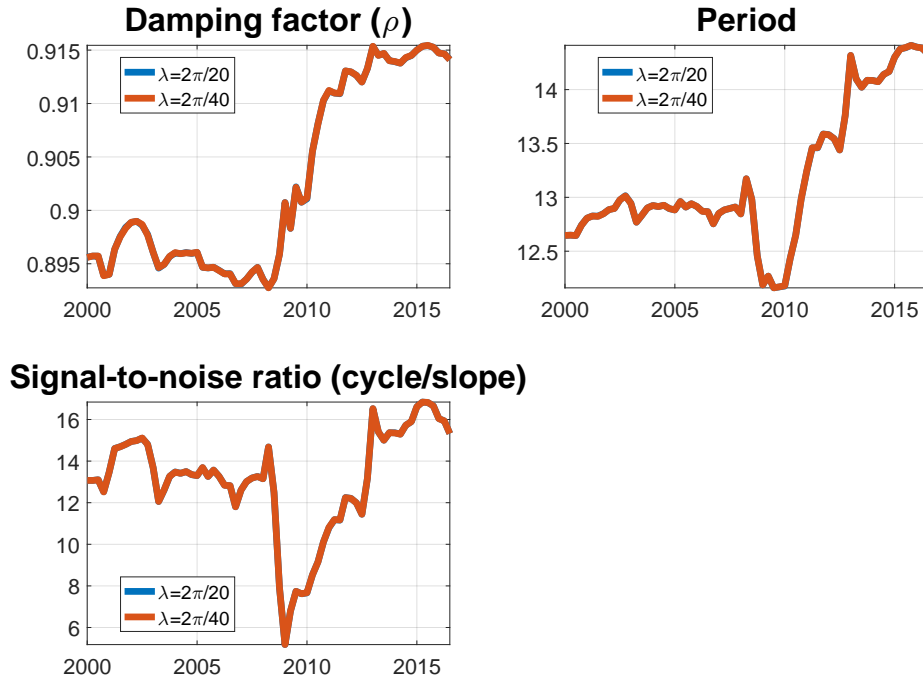
The estimated model is the integrated random walk trend plus stochastic cycle in equations (1)-(2)-(3), without irregular component. The sample period is 1970:Q1-2016:Q3. Two different initial values for the frequency of the cycle λ are considered: $2\pi/20$ and $2\pi/40$. In both cases, the initial value for the damping factor ρ is set at 0.9. The expanding-window estimation starts in 2000:Q1. Then, recursive estimation is performed by adding a quarter at a time, up to 2016:Q3.

Overall the ML estimation of the univariate model for GDP delivers an estimated cycle characterised by relatively short duration and moderate amplitude. These estimates are in line with previous research (see for instance Zizza, 2006) and result in a rather robust (time-invariant) business cycle. Moreover, the slope of the trend component shows evidence of residual cyclicality.

Since an oscillatory slope component (long-run growth rate of potential output) is unreasonable from an economic perspective,[10] in Figure 3 we compare the trend and cyclical components of GDP obtained under maximization of the likelihood with an alternative estimate obtained by calibrating the standard deviation of the slope innovations: this calibration delivers a smoother long-run growth rate of potential output. In particular, we restrict σ_ζ^2 (blue line) such that the signal-to-noise ratio $\frac{\sigma_\kappa^2}{\sigma_\zeta^2}$ is approximately equal to 50 (note that in this case the estimated period is ≈ 39 quarters).[11] The red line instead refers to the estimated value of unrestricted model in Figure 1, yielding $\frac{\sigma_\kappa^2}{\sigma_\zeta^2} = 4$ and the estimated period approximately equal to 14 quarters. For comparison purposes, we also report the trend and cycle produced by the HP filter (green line).

As the slope innovations variance is decreased, the trend component becomes progressively smoother and cyclical fluctuations more pronounced. In this way, it is possible to obtain cycle estimates that feature greater amplitude and duration. As a result, in Figure 3 the stochastic slope component delivered by the calibrated model changes very gradually over time, therefore providing a more reasonable estimate of potential growth. At the same time, the cyclical component at the end of the sample is still negative, in line with the evidence of persistent slack in the economy as suggested by recent unemployment and inflation developments.[12]

---

[10]The growth rate of potential output should be as smooth as possible.

[11]We tried different calibrations and finally chose the one that, in our view, delivers a plausible long-run growth rate of real GDP.

[12]See Banca d'Italia (2016).

Figure 3: Real GDP: Cycle and slope smoothed estimates with different calibrations of the signal-to-noise ratio
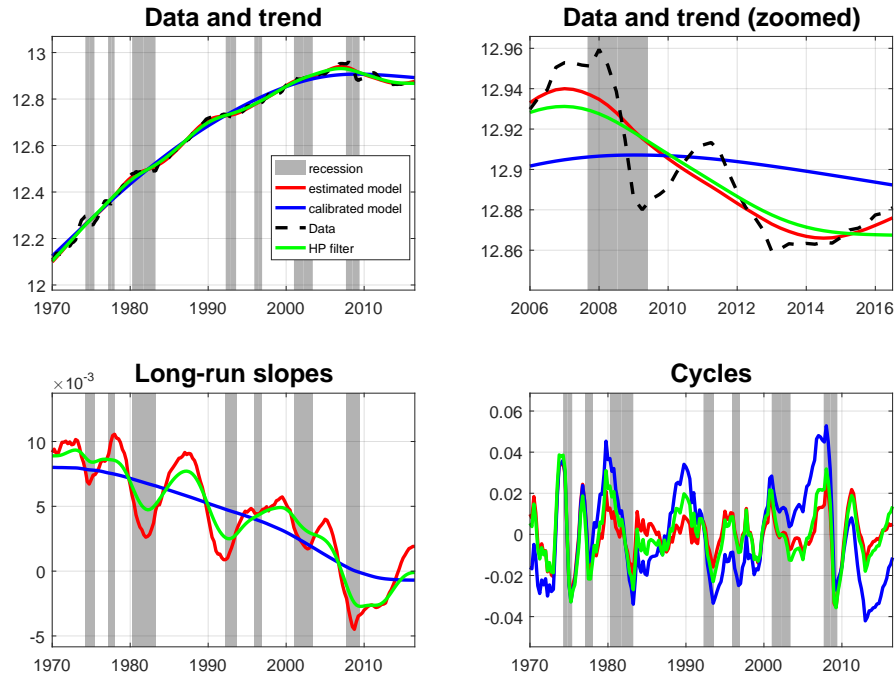

The red line is the estimated model (1)-(2)-(3), without irregular component. The sample period is 1970:Q1-2016:Q3. The blue line represents the same model in which σ_ζ is calibrated such that $\frac{\sigma_\kappa}{\sigma_\zeta} \approx 35$ (the estimated period is ≈ 39). The green line represents the HP filter.

In the remainder of this section, after analysing the results of a univariate trend-cycle decomposition applied to real credit and characterising the financial cycle, we will investigate if a bivariate model that allows for interactions between the real and financial cycles is able to deliver a trend-cycle decomposition of GDP closer to the calibrated one.

3.2 Univariate trend-cycle decompositions for credit

We now turn the focus to credit. We estimate the univariate local linear trend model plus stochastic cycle in equations (1)-(2)-(3) to total credit to the private sector. The sample period is 1970:Q1-2016:Q3. The data source is the Bank of International Settlements (2016) database. The time series is converted into real terms using the GDP deflator.

Figure 4: Real credit: Profile of the log-likelihood as a function of the cycle period ($2\pi/\lambda$)
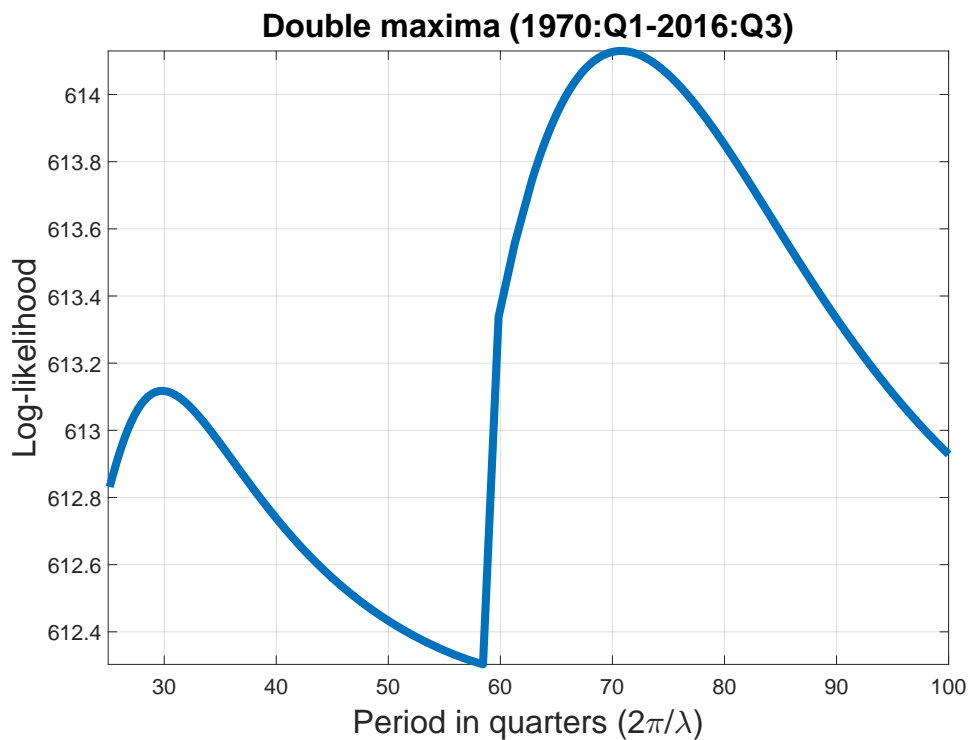
The estimated model is (1)-(2)-(3) over the sample period 1970:Q1-2016:Q3.

Figure 4 shows a slice of the likelihood as a function of the period ($2\pi/\lambda$). Clearly two maxima exist and the associated parameter values depend on the initial conditions. However, a value of λ corresponding to a period of around 70 quarters maximizes the

likelihood globally. A second local maximum appears on the left, corresponding to a period of 30 quarters.

A similar picture emerges in Figure 5, which shows a slice of the likelihood function as a function of the damping factor ρ. Also in this case a global maximum can be identified for values of ρ close to 0.99, while a local maximum occurs at $\rho \approx 0.93$.

**Figure 5: Real credit: Profile of the log-likelihood as a function of the damping factor (ρ)**
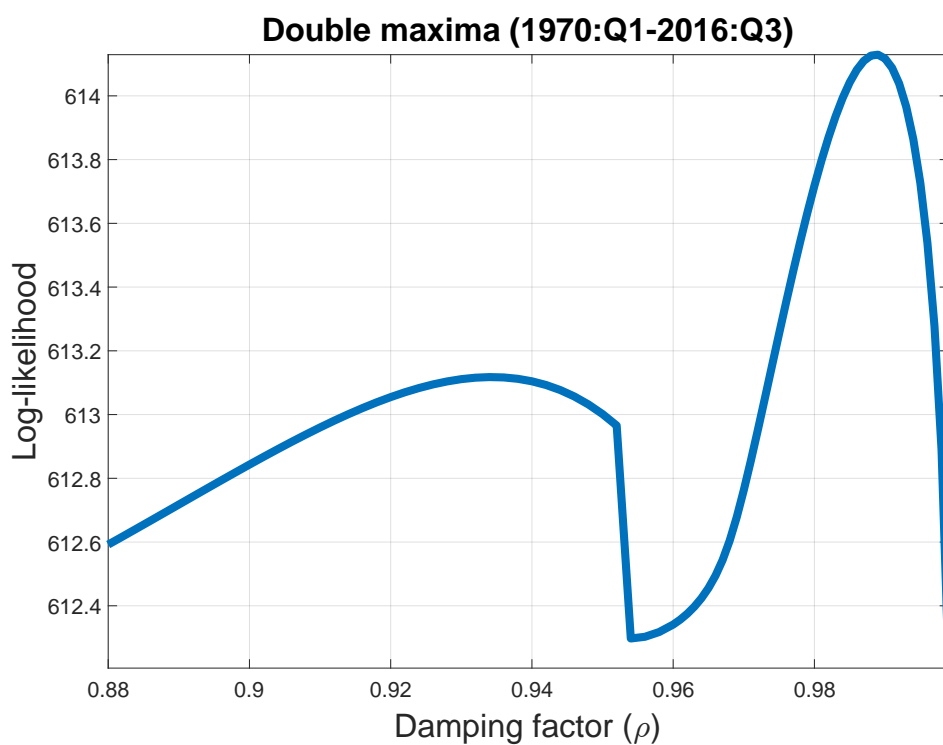
The estimated model is (1)-(2)-(3) over the sample period 1970:Q1-2016:Q3.

In order to shed further light on the shape of the likelihood function, Figure 6 (top panel) shows its three-dimensional plot as a function of the cycle frequency (λ) and the damping factor (ρ). Two maxima are clearly visible in the graph: one is located in a region

in which ρ is close to 0.93 and the period is comprised between 30 and 35 quarters. The other one is on the right-hand corner, where ρ is close to 0.99 and the period is around 70 quarters. Figure 6 (bottom panel) shows the three-dimensional plot from directly overhead, providing an even more immediate visual insight about the precise location of both maxima.

Figure 6: Real credit: Three-dimensional log-likelihood plot as a function of cycle frequency (λ) and damping factor (ρ)
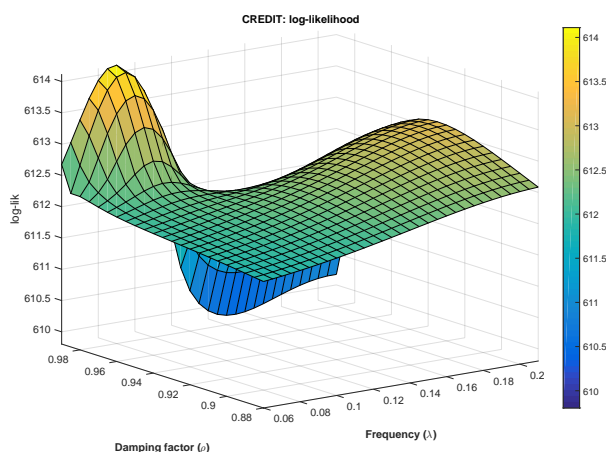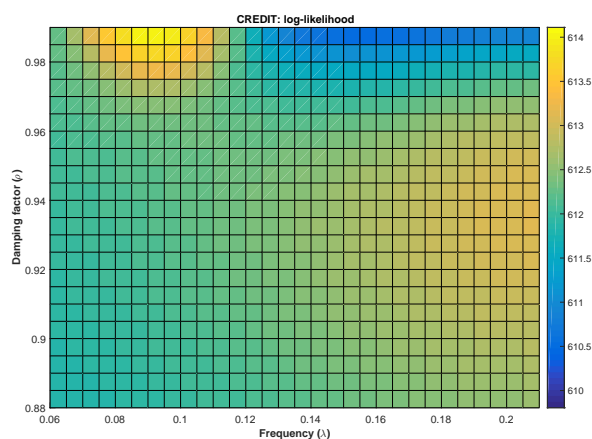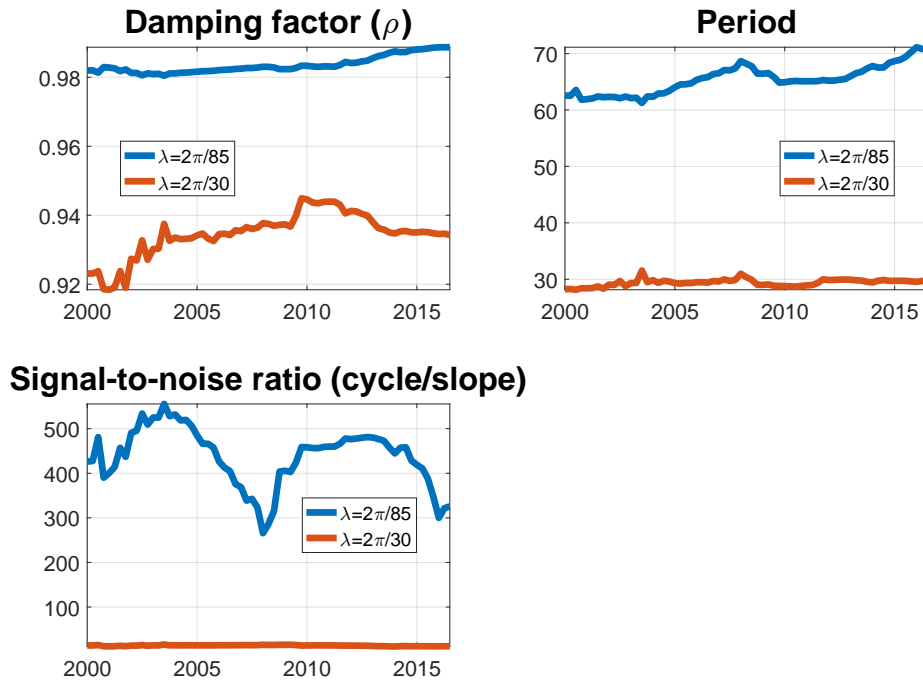

(a) 3d-plot

(b) 3d-plot from directly overhead

As in the case of GDP, we investigate whether our findings are driven by the specific sample considered or are a stable feature of credit data. To this end we consider an expanding estimation window scheme (Figure 7).

**Figure 7: Real credit: Parameter instability analysis based on an expanding estimation window**

The estimated model is (1)-(2)-(3) over the sample period 1970:Q1-2016:Q3. Two different initial values for the frequency of the cycle λ are considered: $2\pi/30$ and $2\pi/85$. In both cases, the initial value for the damping factor ρ is set at 0.9. The expanding-window estimation starts in 2000:Q1. Then, recursive estimation is performed by adding a quarter at a time, up to 2016:Q3.

The expanding-window estimation starts in 2000:Q1. Two different initial values for the frequency of the cycle λ are considered: $2\pi/30$ and $2\pi/85$. The initial value for the damping factor ρ is always set at 0.9. The estimation procedure delivers two different

parameter estimates consistent with the full sample analysis: if the initial value for λ is set to $2\pi/85$, the estimated ρ is close to 0.98-0.99, and the estimated period is around 70 quarters; the signal-to-noise ratio is larger than 400. On the other hand, if the initial value for λ is set to $2\pi/30$, the resulting ρ is comprised between 0.92 and 0.94, while the period is close to 30 quarters and the signal-to-noise ratio (cycle/slope) is less than 20. The influence of initial conditions on λ is quite uniform over the entire sample, the recursive exercise is consistent with the full sample analysis and clearly points to the presence of two maxima of the likelihood function.

Having established the existence of two maxima, we now describe the main features of the corresponding cycles and trends. Figure 8 shows the estimates of trend, slope and cyclical components, along with the 95% confidence intervals, obtained by the Kalman filter and smoother. In this case the initial value of the period $(2\pi/\lambda)$ for ML estimation is 40 quarters (10 years), and the resulting estimate is approximately 30 quarters (almost 8 years). The trend slope is rather erratic and is not as smooth as one would expect from a series that should only include a pure long-term variation. The cycle is also very volatile and its dynamics is difficult to interpret.
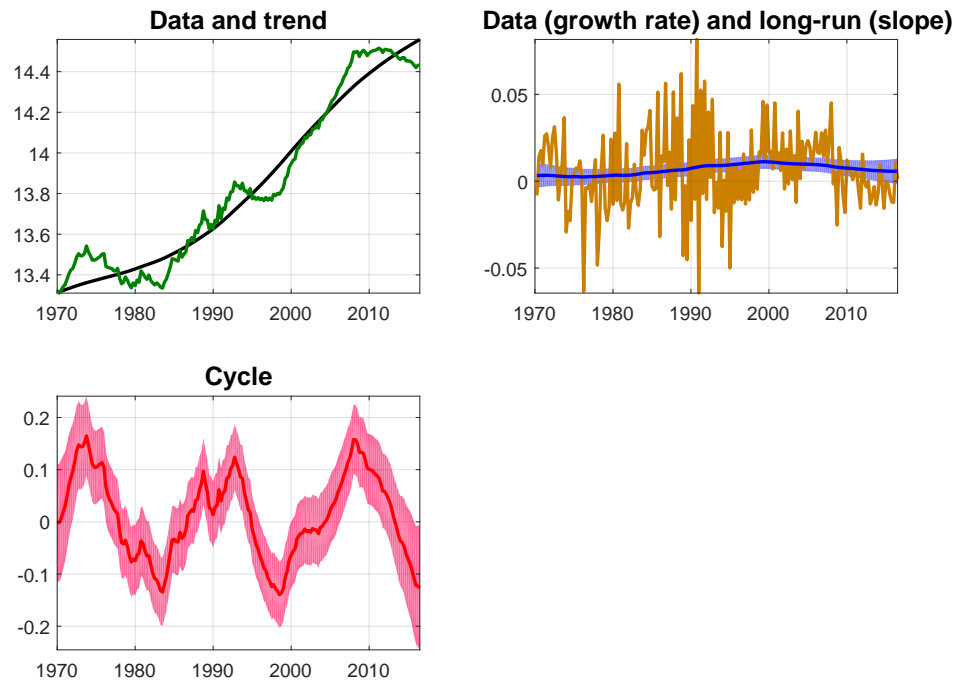
Figure 8: Real credit: Smoothed estimates of trend, slope and cycle (short cycle)
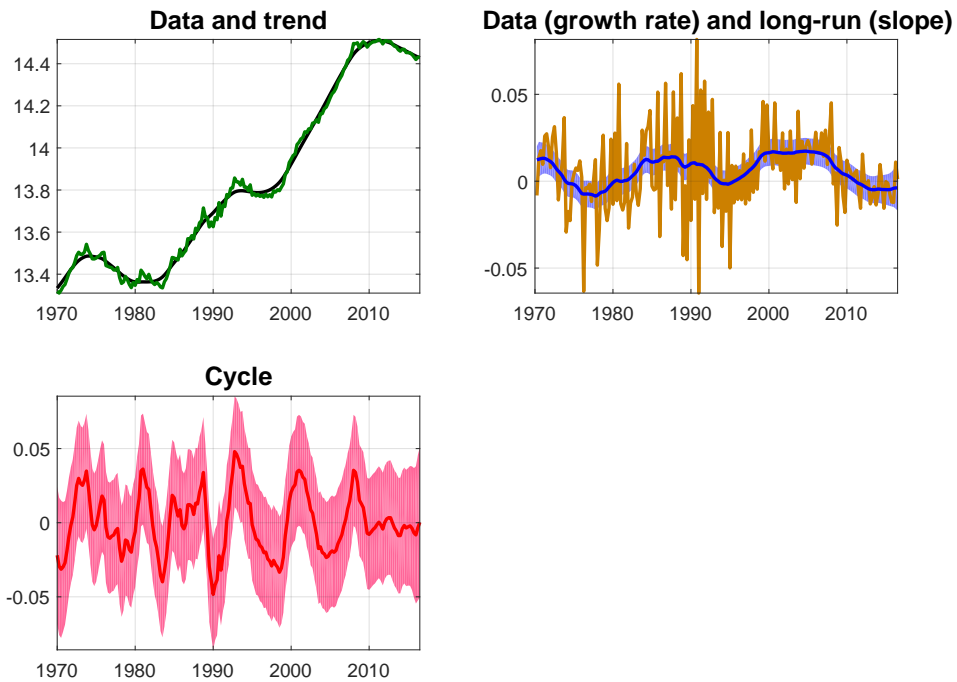
The estimated model is (1)-(2)-(3) over the sample period 1970:Q1-2016:Q3. The first graph on the top left displays the data (in levels) and the estimated trend. The first graph on the top right shows the data in first differences (quarterly growth rate) and the estimated slope with 95% confidence intervals. The bottom panel displays the estimated cycle with 95% confidence intervals. The initial value for the period $(2\pi/\lambda)$ is 40 quarters (10 years).

A different picture can be obtained by setting the initial value for the period $(2\pi/\lambda)$ to 85 quarters (21 years), which leads to an estimated period of roughly 70 quarters (almost 18 years). The resulting trend-cycle decomposition is reported in Figure 9. In general, the trend (slope) component changes very slowly over time and is characterised by three distinct phases: the first one of low but slowly increasing trend growth before the euro adoption, a second one of higher and stable trend growth up to 2009, and a third one of decreasing trend growth after 2009.

Figure 9: Real credit: Smoothed estimates of trend, slope and cycle (long cycle)

The estimated model is (1)-(2)-(3) over the sample period 1970:Q1-2016:Q3. The first graph on the top left displays the data (in levels) and the estimated trend. The first graph on the top right shows the data in first differences (quarterly growth rate) and the estimated slope with 95% confidence intervals. The bottom panel displays the estimated cycle with 95% confidence intervals. The initial value for the period $(2\pi/\lambda)$ is 85 quarters (21 years).

In Figure 9 the cyclical component has a wider amplitude and a much longer duration than the one displayed in Figure 8. Its dynamics appears to be broadly consistent with the historical evidence for Italy. Since 1970, only two complete cycles occurred (from peak to peak); the third one, which started in 2009 is still underway. A lending boom is visible in the early 1970s; then, in the mid-1970s, Italy entered a phase of credit contraction: this is in accordance with the fact that, in those years, credit ceilings were introduced to steer monetary policy. Between the mid-1980s and the first 1990s, Figure 9 shows an

acceleration in total credit. A cycle peak seems to be present between 1992 and 1993. Soon afterwards, a phase of credit contraction occurred: indeed, the main Southern banks were hit by the 1992 crisis, when Italy was forced to leave the European Monetary System (De Bonis and Silvestrini, 2014). Afterwards, a long credit expansion took place, lasting until 2008. The situation changed drastically at the end of 2008, when most of the advanced economies were hit by the global financial crisis. At the end of the sample, the deviation of credit from its long-run trend is still largely negative and close to -10%, in line with the official estimates produced by the Bank of Italy.[13]

3.3 Multivariate trend-cycle decomposition

In this section we estimate a bivariate model for real GDP and real credit over the full-sample 1970:Q1-2016:Q3. As the univariate analysis clearly points out, the business and the financial cycle are remarkably different, therefore we do not impose similar cycle restrictions. The resulting cyclical components therefore differ from the univariate ones, see equation (13). However, we allow for cross-correlations as well as phase shifts between cycles. As a matter of fact, while we do not take a stand on which variable is leading which, the financial stability literature suggests some sort of intertemporal correlation between the two cycles.

Figure 10 shows the output of the multivariate trend-cycle decomposition. The estimated credit cycle is very similar to the univariate one and close to -10% at the end of the sample, while the business cycle shows longer and sharper fluctuations.[14]

---

[13]For the underlying methodology, we refer to Alessandri et al. (2015).

[14]This is mainly due to the fact that the volatility of $\psi_{2,t}$ (measured by the signal-to-noise ratio) is much higher than the volatility of $\psi_{1,t}$. Specifically, small values of a_{12} and a_{12}^* convey a significant impact of $\psi_{2,t}$ on $\tilde{\psi}_{1,t}$, while the coefficients a_{21} and a_{21}^* need to have higher magnitude in order to induce a sizeable impact of $\psi_{1,t}$ on $\tilde{\psi}_{2,t}$. In terms of estimates, we obtain that $a_{12} \approx a_{21} \approx 0$ while $a_{12}^* > a_{21}^*$.

Figure 10: Real and financial cycles smoothed estimates: Output of the multivariate model
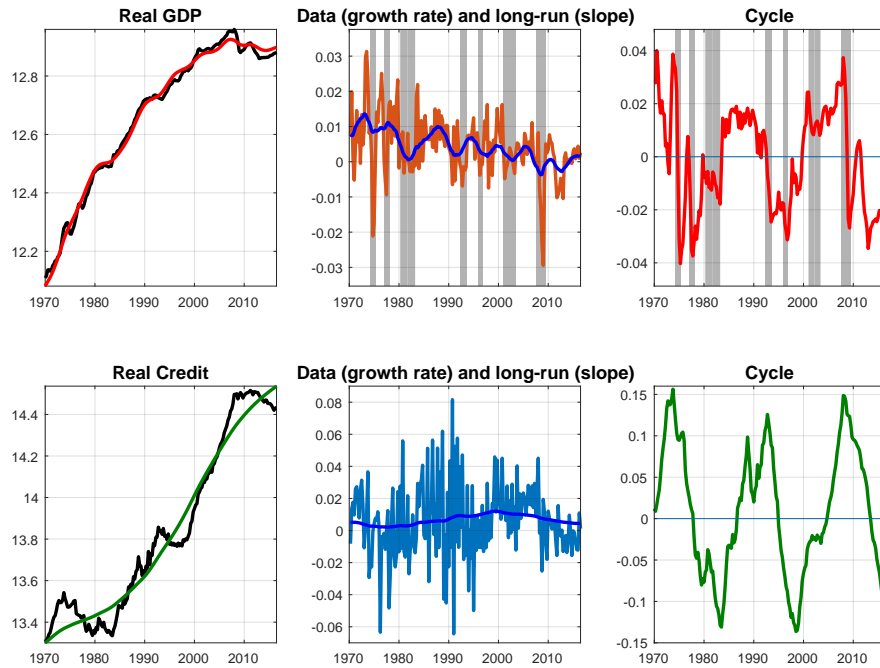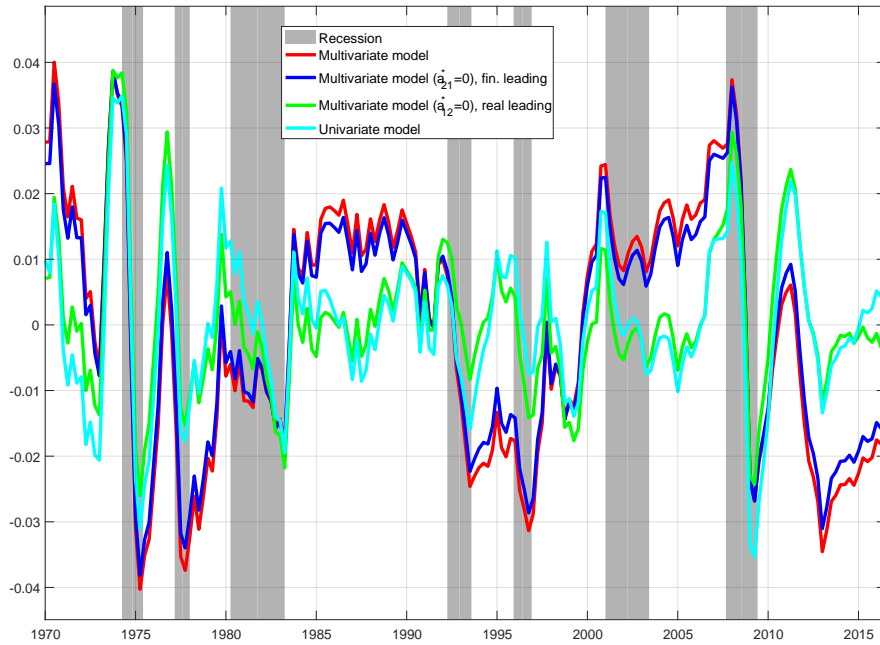

The estimated model is the multivariate integrated random walk trend plus stochastic cycle in equations (6)-(7)-(8)-(9). The sample period is 1970:Q1-2016:Q3.

Figures 11 and 12 allow to better appreciate the difference between the univariate and the multivariate decompositions. Focusing on the business cycle, in the figures we report the univariate cycle (light blue line) and three multivariate decompositions that differ among themselves for the degree of interconnectedness between the real and financial cycles: one model (green line) allows for the business cycle to affect (with lags) the financial cycle. Not surprisingly, the resulting business cycle (green line) closely matches the univariate one. On the contrary, the second model allows for the financial cycle to affect the business cycle, and the resulting cycle differs from the univariate one. In particular, the business cycle (dark blue line) is deeper and longer than the univariate one, suggesting

that financial boom and bust may have a significant impact on economic activity (Silvestrini and Zaghini, 2015). Finally, the unrestricted multivariate model, which delivers the highest log-likelihood, allows both for feedback from the financial to the business cycle and vice versa. The resulting cycle (red line) shows slightly deeper fluctuations than the previous one, suggesting that the full interaction between financial and business cycle tends to further amplify the business cycle. This points at the existence of a financial accelerator mechanism, for which the phases of the two cycles feed into each other with magnifying effects on the amplitude of the swings in economic activity. This mechanism is particularly strong following the euro-area sovereign debt crisis, when the red line clearly signals a much wider output gap than the one obtained from the univariate model. At the end of the sample period (2015-2016) the estimate of the output gap produced by the unrestricted multivariate model is negative and lower than the corresponding univariate estimate (the difference between the two is about 2%).

Figure 11: Real cycle: a comparison of univariate and multivariate models

The estimated univariate model is in (1)-(2)-(3). The estimated multivariate model is in (6)-(7)-(8)-(9). For real GDP, the model is estimated without the irregular component. The sample period is 1970:Q1-2016:Q3.

Figure 12: Real trend and cycle: a comparison of univariate and multivariate models
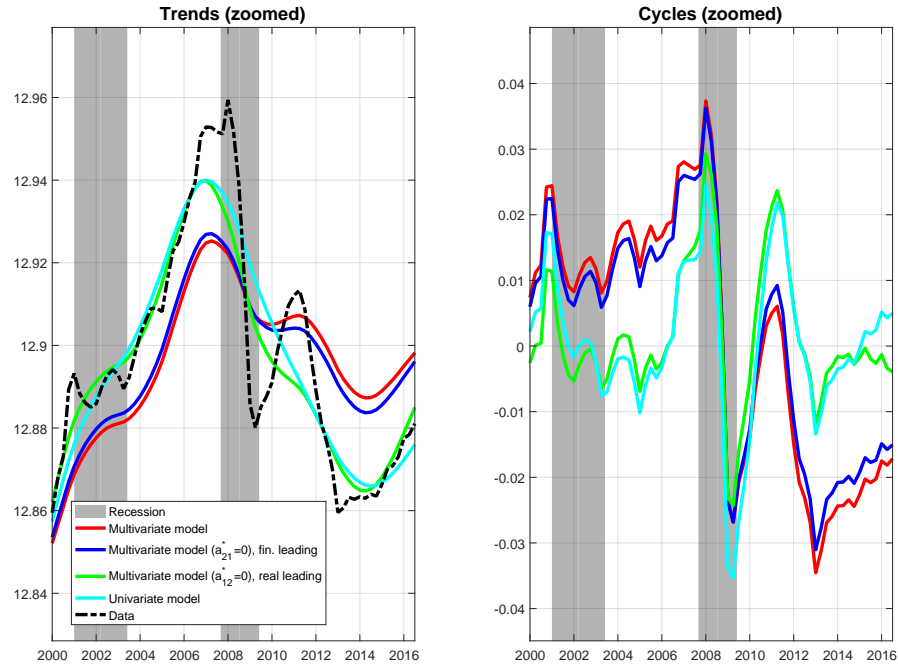
This plot shows estimates of the trend (potential output) and cycle (output gap) from 2000 onwards. The estimated univariate model is in (1)-(2)-(3). The estimated multivariate is in (6)-(7)-(8)-(9). For real GDP, the model is estimated without the irregular component. The sample period is 1970:Q1-2016:Q3.

4 Conclusions

In this paper we have examined the empirical properties of real and financial cycles in Italy through the lenses of unobserved component models. Univariate trend-cycle decompositions deliver a short cycle of approximately 14 quarters for real GDP and two longer cycles of around 30 and 70 quarters for real credit to the private sector. The multivariate model allows to exploit the rich stochastic structure introduced by cross-correlations at leads and lags between real and financial cycles. The presence of these feedback effects results in much wider real cyclical fluctuations than those emerging from the univariate

models. In addition, the financial cycle appears to contain forecasting power for the business cycle. By contrast, the cyclical fluctuations of GDP exert less impact on the credit cycle, which results to be very similar to that obtained by the univariate specification. Finally, the inclusion of the financial variable in the multivariate specification leads to a negative estimate of the output gap in 2015-2016, which is roughly 2% lower than the corresponding univariate estimates.

In this paper we have focused on the connection between real activity and real credit volume. Two natural extensions with additional variables come to mind. First, we could include nominal variables such as the inflation rate in order to reproduce Phillips-curve dynamics. Second, we could introduce foreign determinants of cyclical fluctuations, which an important strand of literature has pointed out as key drivers of financial cycles (Rey, 2013). We leave all these extensions to future research.

References

[1] Aikman, D., Haldane, A., and B. Nelson (2015). Curbing the credit cycle. *Economic Journal*, vol. 125(585), pp. 1072–1109.

[2] Alessandri, P., P. Bologna, R. Fiori and E. Sette (2015). A note on the implementation of a countercyclical capital buffer in Italy, Banca d'Italia, Questioni di economia e finanza (Occasional papers), 278.

[3] Bank of International Settlements (2016). Long series on total credit to the non-financial sectors. Retrieved from http://www.bis.org/statistics/totcredit.htm.

[4] Banca d'Italia (2016). Economic Bulletin No. 4 2016.

[5] Bartoletto, S., Chiarini, B., Marzano, E., and P. Piselli (2017). Business cycles, credit cycles, and bank holdings of sovereign bonds: historical evidence for Italy 1861-2013. Banca d'Italia. Mimeo.

[6] Bassanetti, A., Caivano, M., and A. Locarno (2010). Modelling Italian potential output and the output gap. Working paper series of the Bank of Italy (Temi di Discussione) no. 771.

[7] Bernanke, B., Gertler, M., and S. Gilchrist (1996). The financial accelerator and the flight to quality. *Review of Economics and Statistics*, vol. 78(1), pp. 1-15.

[8] Borio, C. and P. Lowe (2004). Securing sustainable price stability. Should credit come back from the wilderness? BIS working papers No. 157, Bank for International Settlements.

[9] Borio, C. (2012). The financial cycle and macroeconomics: What have we learnt? BIS Working Papers No. 395, Bank for International Settlements.

[10] Borio, C. (2017). Secular stagnation or financial cycle drag. Keynote speech at the 33rd Economic Policy Conference, 5-7 March 2017, Washington DC.

[11] Bry, G., and C. Boschan (1971). Cyclical analysis of time series: selected procedures and computer programs. NBER technical paper 20.

[12] Busetti, F., and M. Caivano (2016). The trend-cycle decomposition of output and the Phillips curve: Bayesian estimates for Italy and the Euro area. *Empirical Economics*, vol. 50(4), pp. 1565–1587.

[13] Carvalho, V., Harvey, A. C., and T. Trimbur (2007). A note on common cycles, common trends, and convergence. *Journal of Business & Economic Statistics*, vol. 25(1), pp. 12–20.

[14] Chen, X., A. Kontonikas, and A. Montagnoli (2012). Asset prices, credit and the business cycle. *Economic letters*, vol. 117(3), pp. 857–861.

[15] Christiano, L., and T. Fitzgerald (2003). The band-pass filter. *International Economic Review*, vol. 44(2), pp. 435–465.

[16] Claessens, S., Kose, M. A., and M. E. Terrones (2012). How do business and financial cycles interact? *Journal of International Economics*, vol. 87(1), pp. 178–190.

[17] De Bonis, R., and A. Silvestrini (2014). The Italian financial cycle: 1861-2011. *Cliometrica*, vol. 8(3), pp. 301–334.

[18] Drehmann, M., Borio C., and K. Tsatsaronis (2012). Characterizing the financial cycle: don't lose sight of the medium term! BIS Working Papers No. 380, Bank for International Settlements.

[19] Drehmann, M. and K. Tsatsaronis (2014). The credit-to-GDP gap and countercyclical capital buffers: Questions and Answers, BIS Quarterly Review, March, pp. 55-73.

[20] Durbin, J., and S. J. Koopman (2001). *Time Series Analysis by State Space Methods*. Oxford: Oxford University Press.

[21] English, W., Tsatsaronis, K., and E. Zoli (2005). Assessing the predictive power of measures of financial conditions for macroeconomic variables. BIS paper no. 22, pp. 228–252, Bank for International Settlements.

[22] Galati, G., Koopman, S. J., Hindrayanto, I., and M. Vlekke (2016). Measuring financial cycles with a model-based filter: empirical evidence from the United States and the euro area. *Economics Letters*, vol. 145(C), pp. 83-87.

[23] Harvey, A. C. (1989). *Forecasting Structural Time Series and the Kalman Filter*. Cambridge: Cambridge University Press.

[24] Harvey, A. C., and A. Jaeger (1993). Detrending, stylized facts and the business cycle. *Journal of Applied Econometrics*, vol. 8(3), pp. 231–47.

[25] Harvey, A. C., and S. J. Koopman (1997). Multivariate structural time series models. In C. Heij, J.M. Schumacher, B. Hanzon and C. Praagman (eds.), *System Dynamics in Economic and Financial Models*, Chichester: Wiley and Sons, pp. 269–298.

[26] Harvey, A. C., and T. Trimbur (2003). General model-based filters for extracting cycles and trends in economic time series. *The Review of Economics and Statistics*, Vol. 85(2), pp. 244–255.

[27] Hatzius, J., Hooper, P., Mishkin, F., Schoenholtz, K., and M. Watson (2010). Financial conditions indexes: A fresh look after the financial crisis. NBER working papers, no. 16150.

[28] Kalman, R. E. (1960). A new approach to linear filtering and prediction problems. Transactions of the ASME, *Journal of Basic Engineering*, 82, pp. 94–135.

[29] Kalman, R. E., and R. S. Bucy (1961). New results in linear filtering and prediction theory. Transactions of the ASME, *Journal of Basic Engineering*, 83, pp. 95–107.

[30] Ng, T. (2011). The predictive content of financial cycle measures for output fluctuations. BIS Quarterly Review, June, pp. 53–65.

[31] Rey, H. (2013). Dilemma not trilemma: The global financial cycle and monetary policy independence. Federal Reserve Bank of Kansas City, Proceedings - Economic Policy Symposium - Jackson Hole.

[32] Rünstler, G. (2004). Modelling phase shifts among stochastic cycles. *Econometrics Journal*, vol. 7(1), pp. 232–248.

[33] Rünstler, G., and M. Vlekke (2016). Business, housing and credit cycles. Working Paper Series, No 1915, European Central Bank, Frankfurt am Main, June.

[34] Schularick, M., and A. Taylor (2012). Credit booms gone bust: Monetary policy, leverage cycles, and financial crises, 1870-2008. *The American Economic Review*, vol. 102(2), pp. 1029–61.

[35] Silvestrini, A. and A. Zaghini (2015). Financial shocks and the real economy in a nonlinear world: from theory to estimation. *Journal of Policy Modeling*, vol. 37, pp. 915–929.

[36] Summers, L. H. (2014). U.S. economic prospects: Secular stagnation, hysteresis, and the zero lower bound. *Business Economics*, vol. 49(2), pp. 65–73.

[37] Zizza, R. (2006). A measure of output gap for Italy through structural time series models. *Journal of Applied Statistics*, vol. 33(5), pp. 481–496.